

Submitted: February 15, 2024

Revised: September 23, 2024

Accepted: October 10, 2024

Numerical and experimental study of the effect of adhesive quality on the repair efficiency of corroded and cracked aluminum plate under mechanical loading

M. Berrahou¹✉, M. Zahraoui^{1,2}, S. Djabbar¹, H. Kamel¹, H. Benzinab¹

¹ University of Relizane, Relizane, Algeria

² Université Oran, Oran, Algeria

✉ berrahou22@yahoo.com

ABSTRACT

A corroded aluminum plate with an inclined crack at the corrosion end was repaired by boron/epoxy composite patches, bonded with various adhesive types under mechanical loads. The aim of this study was to discover which glue types are better for the composite patch adhesive and the most efficient in transferring stresses from the aluminum plate to the patch, so in this study three-dimensional finite element analysis was used to study the changes in the damaged area of the adhesive (DR) and the stress factor (SIF) in the two modes (mode I K_I and mode II K_{II}), then compare them. To confirm the analytical results, we conducted a laboratory experiment using corroded aluminum plate 2024 with random cracks that were repaired with a composite patch affixed with several adhesive types, and then we calculated the ultimate tensile strength. The obtained results, both on the analytical and experimental side, showed that the adhesive type FM73 is more efficient in fixing the composite patch and more effective in transferring stress from the damaged plate towards the patch compared to the other materials used in this study (araldite, adekit and redux).

KEYWORDS

composite • corrosion • mixed mode • stress intensity factor • SIF • damaged area ratio • DR • ultimate tensile strength

Acknowledgements. *The authors extend their sincere thanks to the staff of the Materials Laboratory of Sidi Bel Abbes University for their assistance in carrying out the laboratory experiments for the preparation of this manuscript.*

Citation: Berrahou M, Zahraoui M, Djabbar S, Kamel H, Benzinab H. Numerical and experimental study of the effect of adhesive quality on the repair efficiency of corroded and cracked aluminum plate under mechanical loading. *Materials Physics and Mechanics*. 2024;52(5): 83–100.

http://dx.doi.org/10.18149/MPM.5252024_9

Introduction

The appearance of cracks in a metal structure in any field such as aviation structures and marine structures is a major concern for maintenance operators and a real threat of structural damage [1].

Composite patches have become widely used to repair metal structures that have been damaged due to fatigue or external stresses whether mechanical or thermal. These patches make it possible to delay the spread of cracks and thereby increase the life of structures repaired in this way. The mechanical properties of these repaired structures have been studied in several articles. The influence of several parameters on crack propagation behavior has been carefully studied by several researchers. For example, the effect of composite patch size [2,3], number of layers [4], asymmetry of the repaired structure [5], component tension before bonding of the composite patch [6], incomplete

bonding of the composite patch [7] or residual stresses [8], have been examined in recent literature.

The adhesive plays an important role in the process of repairing damaged structures, it is the mediator between the patch and the plate, and it is responsible for transferring stress from the plate to the patch. The damaged area criterion was proposed by [9,10] for the analysis of damage in the adhesive. This standard assumes that the material will fail once the measured stress exceeds the ultimate strength of the material. Sheppard and colleagues [10] introduced the idea of a damaged area of an aluminum plate repaired with a single and double composite. This area is determined by a surface, where the von-Mises deformations exceed the maximum permissible deformation, and the fracture load of glue joints was determined experimentally. Damage to the adhesive layer occurs when the strains or stresses in the adhesive are greater than the material properties. Failure in the adhesive is not caused by crack propagation in the substrate, but rather by initiation and propagation of the damaged area in the layer containing defects such as microcracks or voids [11]. The percentage of damaged area has been suggested to predict the load of glue joint failure. For FM73 epoxy adhesive, it has been shown that this adhesive fails when the damaged area ratio reaches the $D_{RC} = 0.247$. In the damaged area theory, it is assumed that the glue joint is non-adherent when the damaged area reaches a certain critical value. The affected area can be determined by either pressure or deformation criterion. The deformation criterion is more appropriate when the adhesive exhibits significant non-linearity. There are two ways for adhesive joints to fail: interface failure and cohesion. In the interfacial mode, the critical failure load of the glue joint is related to the interfacial pressure between the adhesive and the part to be glued [12].

There are several works carried out by M. Berrahou [13–19] to study the repair of plates, whether metal such as aluminum or composite plates using the composite patching technique, and these studies were numerical analytical research and laboratory experiments. In [20–22], it was also showed that the determination of the stress intensity factor on the crack tip is one of the possible ways to analyze the repair performance associated with these composite materials, using the three-dimensional finite element method.

In this work, we place ourselves in the context of a numerical analytical study using the 3D finite element method to assess the damaged area ratio of the adhesive and the intensity of the stress factor at the crack tip, in addition to laboratory experiments to find out the ultimate tensile strength value for each sample. These samples were corroded aluminum plates of type 2024 with random cracks, originally made by boron / epoxy resin bonded with different types of adhesives (FM73, araldite, adekit and redux). The aim of this study was to determine which of these adhesives are more efficient in stress transfer and reduce the risk of repair damage and thus enhance the corrosion resistance properties.

Geometrical model

The geometry of the structure considered in this study is shown in Fig. 1. For a rectangular elastic thin plate of 2024-T3 aluminum with random shaped corrosion, with the following dimensions: $H_{pl} = 254$ mm, $W_{pl} = 254$ mm and $e_{pl} = 5$ mm, with an inclined crack of length $a = 15$ mm. The plate was repaired with a single boron/epoxy patch of different shapes

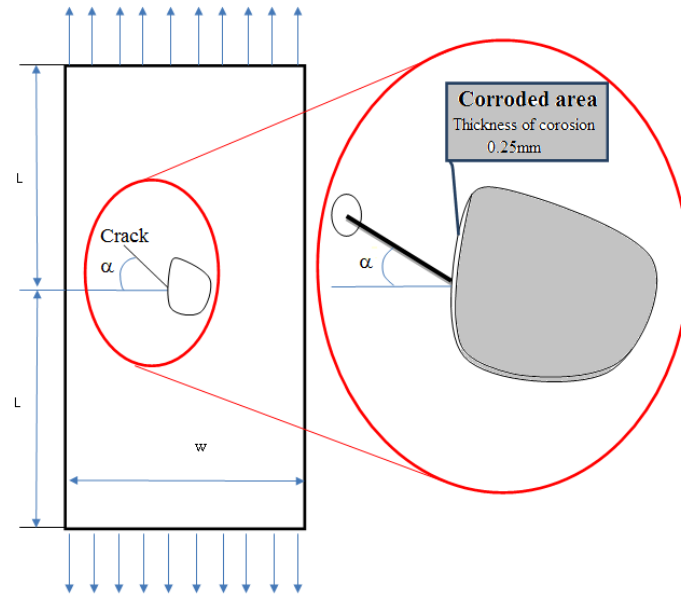


Fig. 1 Geometry of the damaged plate

and constant thickness $e_{\text{pat}} = 1.5\text{ mm}$, the layers in the patch have a unidirectional stacking where the fibers are oriented along the length direction of the specimen (parallel to the load direction). In order to analyze the effect of the type of adhesive, four types of adhesives were chosen in this study: (FM73, adekit A140, redux and araldite). We used four patch shapes in this study: rectangular, trapezoidal, circular and elliptical, having the same surface $A = 9750\text{ mm}^2$. The sizes of these patches are given in Fig. 2. The patch is bonded with 0.15 mm thick adhesive. The plate is subjected to a uniaxial tensile load of amplitude $\sigma = 100\text{ MPa}$ and with an ambient temperature $T = 20\text{ }^\circ\text{C}$.

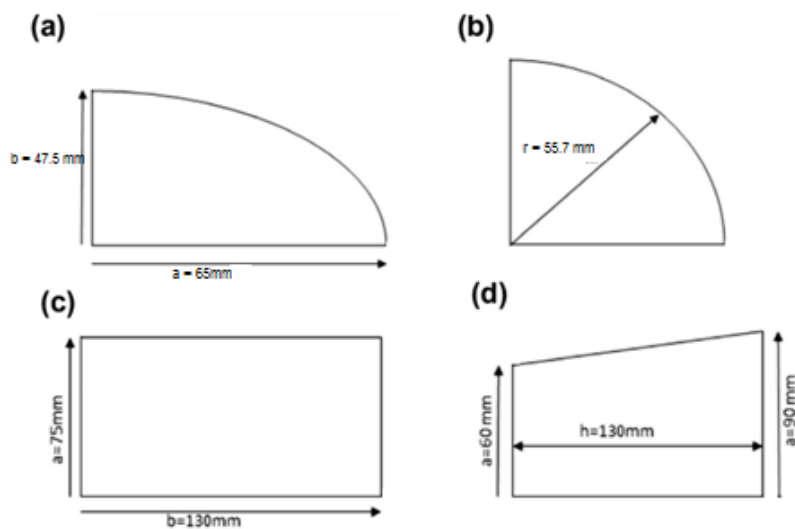


Fig. 2. Patch dimensions: (a) elliptical, (b) circular, (c) rectangular, (d) trapezoidal

The mechanical properties of (the plate, patch and of the adhesive) are shown in Table 1. The geometric shape of the corrosion used is randomly in 3D with a thickness 0.25 mm, before repairing the structure, the corroded area is cleaned to remove the Corrosion film and keep the same mechanical properties.

Table 1. Elastic property of different materials [23]

	Boron/ep	AL 2024	FM 73	Adekit	Redux	Araldite
E_1 , GPa	200	72				
E_2 , GPa	2.5					
E_3 , GPa	2.5					
ν_{12}	0.21	0.33	0.32	0.3	0.36	0.36
ν_{13}	0.21					
ν_{23}	0.21					
G_{12} , GPa	7.2		4.2	2.69	3.808	2.448
G_{13} , GPa	5.5					
G_{23} , GPa	5.5					

Finite element modeling

The analysis involved a three-dimensional finite element method to supplement and analyze the experiments by using a commercially available finite element code ABAQUS [24]. The finite element model consisted of three subsections to model the cracked plate, the adhesive, and the composite. The J integral values were extracted using a domain integral method within ABAQUS. This method provides high accuracy with rather coarse models in three- dimensions. The J integral values were extracted using a domain integral method within ABAQUS. This method provides high accuracy with rather coarse models in three dimensions. To generate crack front some brick elements are replaced by "crack block". These crack-blocks are meshes of brick elements which are mapped into the original element space and merged with surrounding mesh. Boundary conditions and loads are transferred to the crack-block elements. The mesh was refined near the crack-tip area with an element dimension of 0.067 mm using at least 15 such fine elements in the front and back of the crack tip. The finite element mesh was generated using brick elements with 20 nodes. The number of elements used in this analysis is 50000 and number of degrees of freedom DOF is 322016. Figure 3 shows the overall mesh of the specimen and mesh refinement in the crack-tip region.

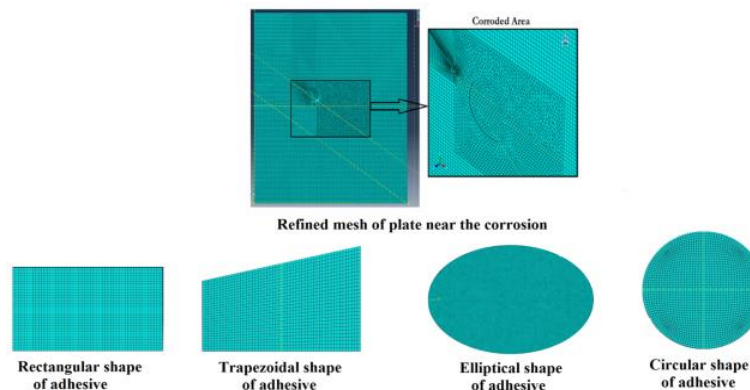


Fig. 3. Typical mesh model of the plate and the patch

Results and Discussions

The von-Mises Failure criterion was introduced by von-Mises (1913) and has been used since as one of the most reliable failure criteria for engineering materials. It relies on the second deviatoric invariant and the effective average stress. Assuming a triaxial test condition where $\sigma_1 > \sigma_2 = \sigma_3$,

$$\sqrt{J_2} = 1/3(\sigma_1 - \sigma_3). \quad (1)$$

The effective average stress can be expressed by the following equation:

$$\sigma_m - P_0 = 1/3(\sigma_1 + 2\sigma_3) - P_0, \quad (2)$$

where P_0 formation pore pressure and the effective average stress is defined as the average stress minus the pore pressure.

In the von-Mises shear criterion, the second deviatoric invariant is plotted against the effective average stress for various axial loads σ_1 and confining pressures σ_3 . The resulting curve, known as the failure curve, specifies two regions, one below the curve as being safe and stable and the other above the curve as being unstable and failed as shown in Fig. 4.

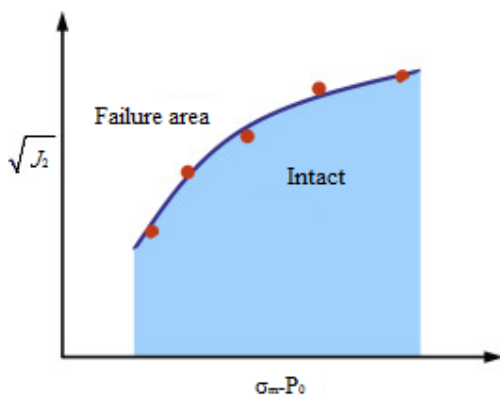


Fig. 4. Von-Mises failure model from triaxial test data

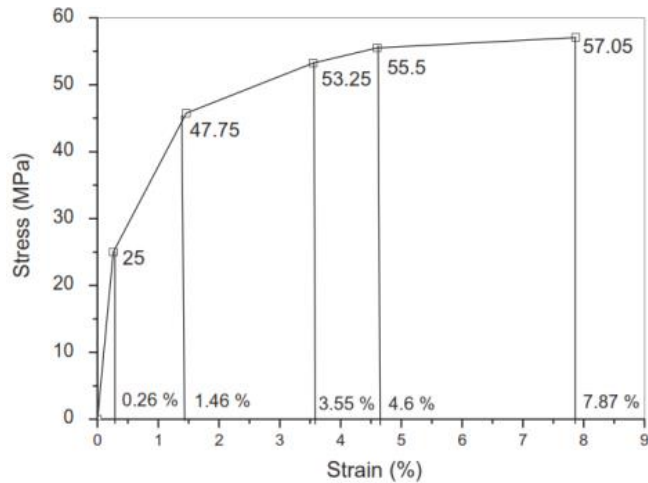


Fig. 5. Stress-strain curve of epoxy adhesive FM73

The theory's Main assumption of is that the adhesive and crack initiation in the bonded patch occurs after a damaged area develops. Under low amplitude of load, the localized damage arrives at the edges of patch. This damage occurs because the material is locally subjected to strains higher than the ultimate material strain. Under medium load amplitude, the damaged zones grow in size and the concentration of points of the damaged areas increases. As the failure load is reached, the damaged area in the adhesive grows to a critical size and the individual components of the damage coalesce and form a crack. Numerically, the damaged area is identified by marking items for which a failure criterion is exceeded. The adhesive tested is a toughened ductile adhesive which is expected to fail in performance. Consequently, the failure criterion used for the cohesive damage of the adhesive layer is the equivalent von-Mises strain criterion:

$$\varepsilon_{equiv} = \frac{1}{\sqrt{2(1+\nu)}} X \sqrt{(\varepsilon_{p1} - \varepsilon_{p2})^2 + (\varepsilon_{p2} - \varepsilon_{p3})^2 + (\varepsilon_{p3} - \varepsilon_{p1})^2}, \quad (3)$$

where ε_{equiv} is the equivalent patches, ε_{pi} are the plastic strains in the different directions and ν is the Poisson ratio.

This criterion is satisfied when the maximum principal strain in the material reaches the ultimate principal strain. For each failure criterion an ultimate strain will be defined and the corresponding damage zone size at failure is determined. The damaged area theory is based on the principle that the adhesive joint is assumed to fail when the damaged area reaches a certain critical value. The damaged zone can be determined by either stress or a strain criterion. Therefore, the adhesive fails to perform its functions when the cohesive failure criterion is satisfied with the adhesive joint. Since adhesive failure occurs at the adhesive joint, the adhesive failure criterion for the damaged area should be used. For isotropic materials, failure criteria such as the von-Mises and Tresca criteria can be used to better understand the adhesive failure. Chang-Su Ban [12] proved that the area where the equivalent strain of the adhesive exceeds the ultimate strain of 7.87 %. After conducting studies on the FM-73 adhesive they concluded that this adhesive fails when the D_R (damaged area ratio) reaches a percentage exceeding 0.24 which is considered critical [25] (Fig. 4). The value of the damaged area ratio is calculated according to the following relationship:

$$D_R = \frac{\text{sum of damaged areas}}{\text{total adhesive area}} \quad (4)$$

In our work, the evaluation of the breaking stress of the FM73 adhesive is calculated from the curve in Fig. 5.

This study was carried out to determine the evolution of the damaged area in the adhesive layer which ensures the adhesion of the composite patch to the cracked plate with randomly shaped corrosion. The area of the damaged zone was calculated for different parameters such as the following effects, patch shapes (rectangular, trapezoidal, and circular), patch types (boron/epoxy, graphite/epoxy and glass/epoxy) and crack inclination under thermo-mechanical loading. The damaged area theory was used to evaluate the progression of damage in the adhesive layer during the analysis. The color of the damaged area can be seen in gray.

The criterion of von-Mises is used as criterion of plasticity. The theory of additional plasticity is introduced to model the non-linearity of the adhesive material. The stress intensity factors at the crack tip are calculated using the virtual crack closure technique (VCCT) based on the energy balance. In this technique, the stress intensity factors are obtained for the three failure modes according to the equation:

$$G_i = \frac{K_i^2}{E}, \quad (5)$$

where G_i is the Fracture energy for mode I, K_i is the stress intensity factor for mode i and E is the modulus of elasticity.

The model referred to above is called the linear elastic fracture mechanics model and has found wide acceptance as a method for determining the resistance of a material to below-yield strength fractures. The model is based on the use of linear elastic stress analysis; therefore, in using model one implicitly assumes that at the initiation of fracture any localized plastic deformation is small and considered within the surrounding elastic stress field.

$$\begin{cases} \sigma_x = \frac{K}{\sqrt{2\pi r}} \cos \frac{\theta}{2} \left[1 - \sin \frac{\theta}{2} \sin \frac{3\theta}{2} \right] \\ \sigma_y = \frac{K}{\sqrt{2\pi r}} \cos \frac{\theta}{2} \left[1 + \sin \frac{\theta}{2} \sin \frac{3\theta}{2} \right] \\ \sigma_{xy} = \frac{K}{\sqrt{2\pi r}} \sin \frac{\theta}{2} \left[\cos \frac{\theta}{2} \cos \frac{3\theta}{2} \right] \end{cases} \quad (6)$$

The stress in the third direction are given by $\sigma_z = \sigma_{xz} = \sigma_{yz} = 0$ for the plane stress problem, and when the third directional strains are zero (plane strain problem), the out of plane stresses become $\sigma_{xz} = \sigma_{yz} = 0$ and $\sigma_z = \nu(\sigma_x + \sigma_y)$. While the geometry and loading of a component may change, as long as the crack opens in a direction normal to the crack path, the crack tip stresses are found to be as given by Eq. 6.

The stress intensity factor (K) is used in fracture mechanics to predict the stress state "stress intensity" near the tip of a crack or notch caused by a remote load or residual stresses. It is a theoretical construct usually applied to a homogeneous, linear elastic material and is useful for providing a failure criterion for brittle materials, and is a critical technique in the discipline of damage tolerance. The concept can also be applied to materials that exhibit small-scale yielding at a crack tip.

The magnitude of K depends on specimen geometry, the size and location of the crack or notch, and the magnitude and the distribution of loads on the material. It can be written as [26,27]:

$$K = \sigma \sqrt{\pi a} f\left(\frac{a}{W}\right), \quad (7)$$

where: $f\left(\frac{a}{W}\right)$ is a specimen geometry dependent function of the crack length a , the specimen width W , and σ is the applied stress.

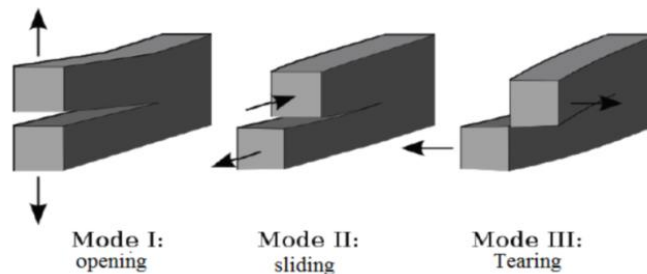


Fig. 6 Mode I, mode II, and mode III crack loading

In 1957, G. Irwin [28] found that the stresses around a crack could be expressed in terms of a scaling factor called the stress intensity factor. He found that a crack subjected to any arbitrary loading could be resolved into three types of linearly independent cracking modes. These load types are categorized as Mode I, II, or III as shown in Fig. 6. Mode I is an opening (tensile) mode where the crack surfaces move directly apart. Mode II is a sliding (in-plane shear) mode where the crack surfaces slide over one another in a direction perpendicular to the leading edge of the crack. Mode III is a tearing (antiplane shear) mode where the crack surfaces move relative to one another and parallel to the leading edge of the crack. Mode I is the most common load type encountered in engineering design.

Different subscripts are used to designate the stress intensity factor for the three different modes. The stress intensity factor for mode I is designated K_I and applied to the crack opening mode. The mode II stress intensity factor K_{II} , applies to the crack sliding mode and the mode III stress intensity factor K_{III} applies to the tearing mode. These factors are formally defined as [29]:

$$\begin{aligned} K_I &= \lim_{r \rightarrow 0} \sqrt{2\pi r} \sigma_{yy}(r, 0), \\ K_{II} &= \lim_{r \rightarrow 0} \sqrt{2\pi r} \sigma_{yx}(r, 0), \\ K_{III} &= \lim_{r \rightarrow 0} \sqrt{2\pi r} \sigma_{yz}(r, 0). \end{aligned} \quad (8)$$

Effect of crack inclination on adhesive damage

This part was carried out in order to determine the development of the damaged area in the adhesive layer due to corrosion. The damaged area theory was used to achieve the objectives of the analysis. The surface of the damaged area was calculated from the adhesive used to repair the damaged plate with random corrosion with a inclined crack at an angle θ for the effects of different types of adhesives and with different patch shapes (rectangular, trapezoidal, circular and elliptical). Where, using the damage area theory, the surface of the damaged areas appears in gray. By calculating the surface of this gray area, the development of damage in the adhesive layer during mechanical loading can be assessed.

This effect is shown on the images in Fig. 7, 9 and 11. This shows the differences in the damaged area of the adhesive as a function of the crack inclination (θ) for a fixed length $a = 15$ mm repaired with a single boron/epoxy patch. We fixed the adhesive thickness $e_{ad} = 0.15$ mm and the thickness of the $ep_{at} = 1.5$ mm, for different patch shapes (rectangle, trapezoid, circle, ellipse) and for an equal applied load at 100 MPa. We changed the crack inclination at angles $\theta = 15, 45, 75^\circ$, after defining the different graphs of the proportion of the damaged area and the curves of variation of the intensity modulus, a comparison can be made between the different types of different adhesives and determine the effect of the crack inclination.

Rectangular Patch

Figure 7 shows the pictorial results that allowed us to follow the development of the damaged area according to the crack inclination. In general, we find that the higher the crack inclination, the smaller the damaged area surface for all adhesive types. In the cases of $\theta = 15^\circ$ and $\theta = 75^\circ$ one notices a damaged area only at the patch periphery. As for the inclination $\theta = 15^\circ$, we notice the appearance of the damaged area around the corrosion and crack.

Figure 8 shows the variance of D_R as a function of the crack inclination θ for different adhesives (araldite, redux, adekit and FM73). All curves have the same behavior, because D_R decreases with the increase in the value of the inclination θ . By comparing the performance through the curves obtained, it can be seen that FM73 adhesive is the most efficient as it gives the lowest D_R values. The least effective for repair is redux adhesive.

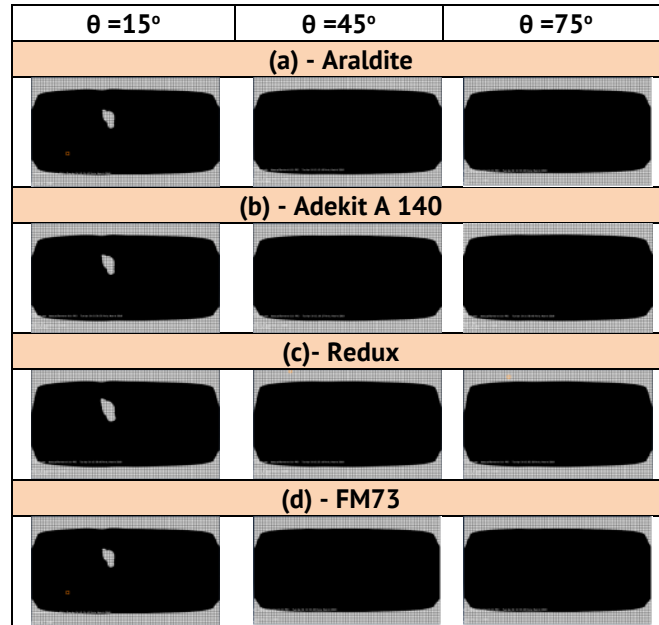


Fig. 7 Damaged area for a patch of rectangular shape and glue (a) araldite, (b) adekit A 140, (c) redux and (d) FM73

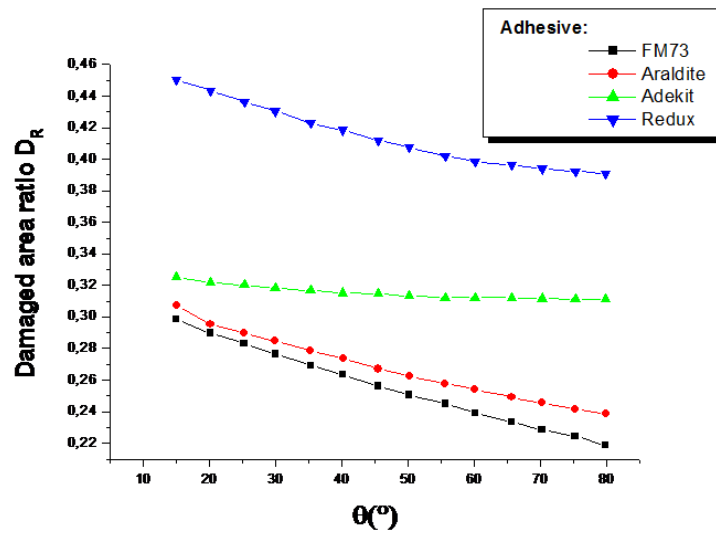


Fig. 8 Variation of D_R ratio for rectangular shape for different adhesives

Trapezoidal patch

Figure 9 represents the results that make it possible to observe the evolution of the damaged area of the adhesive according to the crack inclination. In general, we find a direct proportion between crack inclination and the damaged area of the adhesive, the greater the crack inclination, the greater this damaged area for all types of glue. In all cases, we also note the presence of a damaged area in the patch vicinity only, and the absence of any damage in the vicinity of the corrosion and crack.



Fig. 9 Damaged area for a patch of trapezoidal shape and glue (a) Araldite, (b) Adekit A 140, (c) Redux and (d) FM73

Figure 10 shows the variance of D_R as a function of the crack inclination θ of the different adhesives (araldite, reduce, adekite and FM73). The damaged area of the adhesive (araldite, reduce and adekit) passes a minimum of $\theta=55^\circ$ and then gradually stabilizes after this inclination. Redux glue is the worst among these adhesives because it gives the greatest values for the damaged area ratio. The variance in D_R increases for the FM73 adhesive but with a much lower inclination than for the other three adhesives and at a very small interval of values 0.26 until $D_R = 0.24$ for $\theta=80^\circ$ is reached. It can be concluded that the FM73 adhesive is the most efficient because it gives the lowest D_R values.

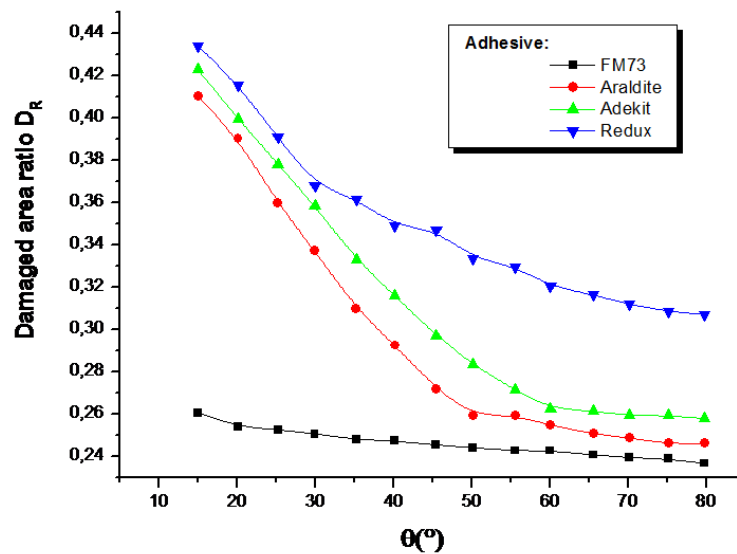


Fig. 10 Variation of D_R ratio for trapezoidal shape for different adhesives

Circular Patch

Figure 11 represents the results that make it possible to follow the development of the damaged area according to the crack inclination in the case of circular patching. In general, we find that the increase in the crack inclination leads to a decrease in the surface of the damaged area of the adhesive. In all cases, we note a damaged area in the patch vicinity. In addition, we observe the appearance of small damaged areas in the corrosion vicinity and crack in this case of araldite, adekit and FM73 for the inclination angle $\theta = 15^\circ$.

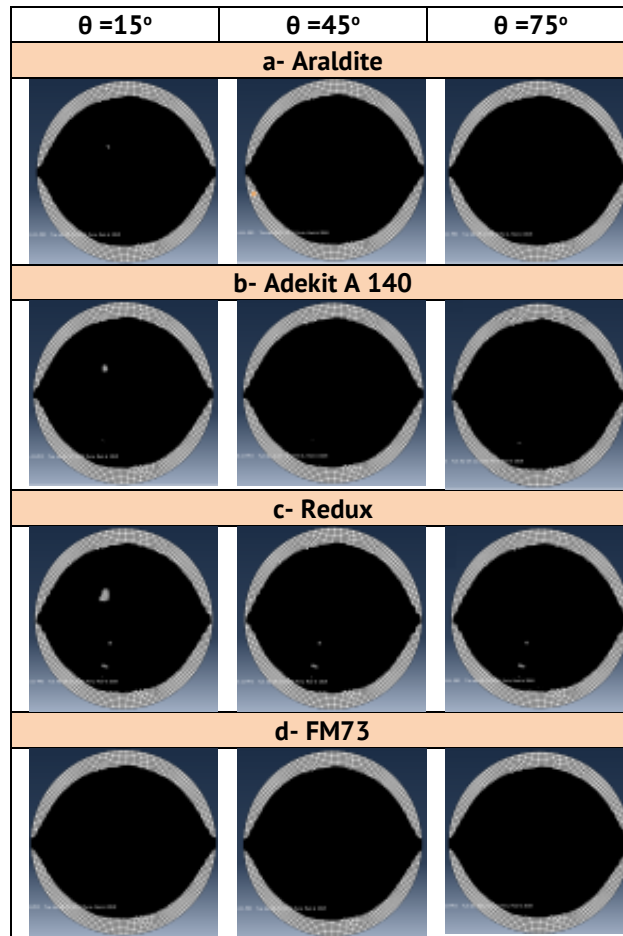


Fig. 11 Damaged area for a patch of circular shape and glue (a) araldite, (b) adekit A 140, (c) redux and (d) FM73

One notes in Fig. 12 the differences in D_R according to the crack inclination θ of different adhesives (araldite, redux, adekit and FM73). The damaged areas of the adhesives (redux and adekit) are noticeably the same for all angles inclinations. The variance of the D_R for the FM73 adhesive decreases but with values much lower than those of the other three adhesives and in an interval of values ranging from 0.21 until reaching $D_R = 0.12$ which is always less than $D_{RC} = 0.247$. We can conclude that FM73 adhesive is the most effective because it gives the lowest D_R values. Araldite is more efficient than adekit and redux.

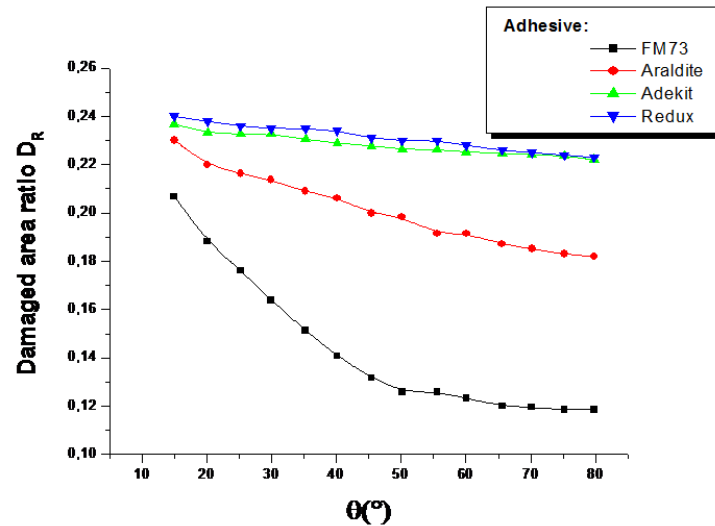


Fig. 12. Variation of D_R ratio for circular shape for different adhesives

Elliptical patch

Figure 13 represents the results that make it possible to follow the development of the damaged area according to the crack inclination in the case of an elliptical patch. In general, we find that as the crack inclination increases, the area of the damaged area of the adhesive decreases. In all cases, we note the presence of a damaged area in the patch vicinity, and the absence of any damage in the vicinity of the corrosion and crack.

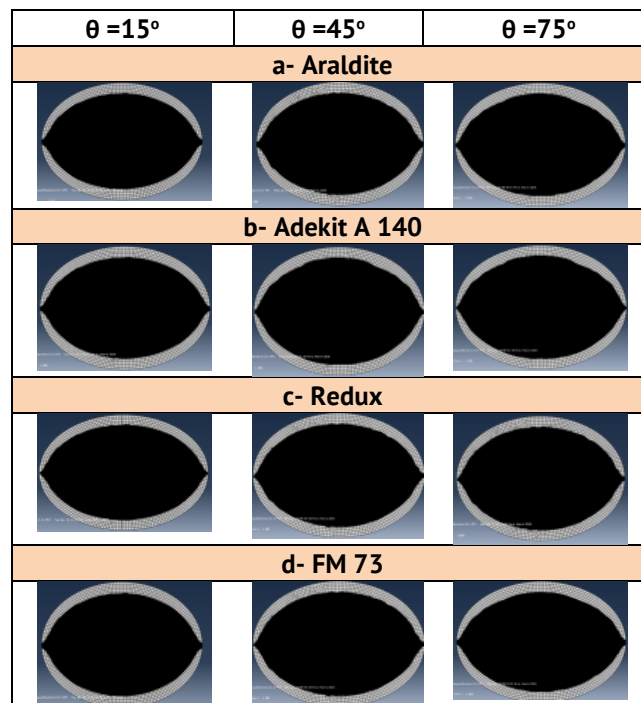


Fig. 13. Damaged area for a patch of elliptical shape and glue (a) araldite, (b) adekit A 140, (c) redux and (d) FM73

We observed in Fig. 14 the variation of D_R according to the crack inclination θ of the different adhesives (araldite, redux, adekit and FM73). The damaged area ratio of adhesives (FM73) is better than that of (adekit, redux and araldite) because their values are the smallest. On the other hand, we conclude for elliptical patch that FM73 glue is the most efficient than other adhesives.

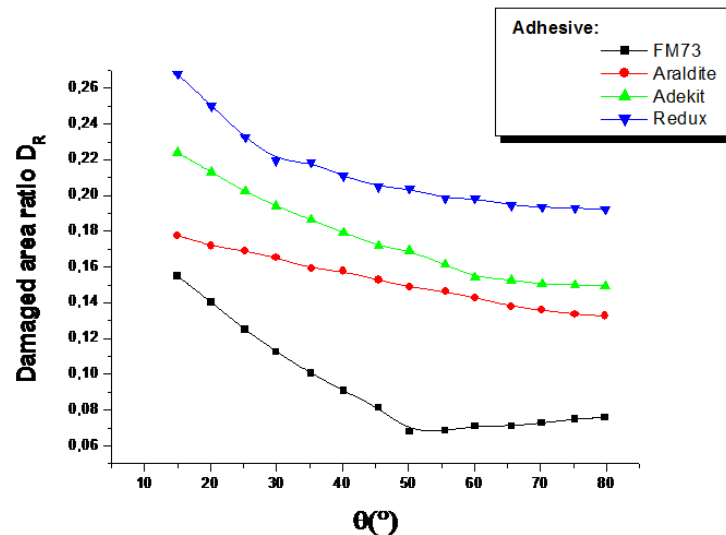


Fig. 14. Variation of D_R ratio for elliptical shape for different adhesives

Stress intensity factor Calculation according to the crack inclination θ

Figures 15-17 present, respectively, the variations of the SIFs in modes I, II and mixed mode (I+II) according to the crack inclination θ for the length crack of 15 mm. We have used in this part of the study the Elliptical-shaped patch, because from the results obtained in the part dedicated to the damaged area of the adhesive or in previous studies we carried out [13,15,17,19], we have confirmed that the elliptical shape gives the best results compared to other shapes (rectangular, trapezoidal and circular).

For mode I

The curves in Fig. 15 present the variations of SIFs according to the crack inclination θ , for a crack with a size $a = 15$ mm in mode I. SIF " K_I " is calculated for four different types of adhesives (araldite, redux, adekit and FM73) used in the installation of the boron/composite patch epoxy and with four shapes (rectangular, trapezoidal, circular and elliptical) according to the crack inclination θ of the crack, Under pressure $\sigma = 100$ MPa and temperature $\Delta t = 20$ °C. The curves presented in Fig. 15 have almost the same behavior, where the decrease in SIF values is related to the increase in the crack inclination for all types of composites used in this study.

As it is clear to us according to all shapes and types of adhesives used that the stress intensity factor is at its maximum when the cracks are perpendicular to the stress, which leads to the largest crack opening at the angle $\theta = 0^\circ$, this behavior is due to the fact that for $\theta = 0^\circ$, The pure mode I exists and therefore the stress absorption by the patch is maximum which increases the patch performance.

The difference in SIF between FM73 and araldite is about 36 % for $\theta = 0^\circ$ and 17 % for adekit and 15 % for redux, this difference tends towards 0 for $\theta = 90^\circ$.

After comparing the results of all curves, it becomes clear to us that the FM73 type adhesive is the most efficient compared to the other adhesives, because it gives the lowest values for the stress intensity factor in all patch shapes.

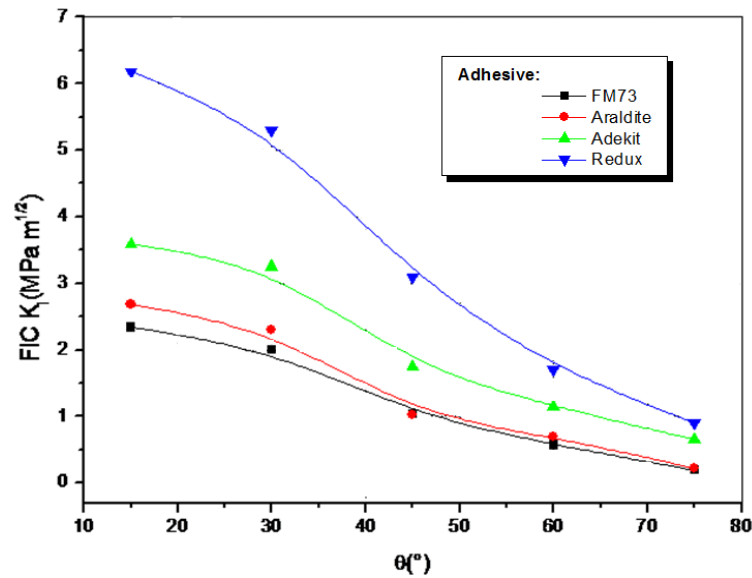


Fig. 15 SIF vs the crack inclination θ of mode I for elliptical shape patch

For mode II

Figure 16 shows that the SIF (K_{II}) differences in Mode II are affected by the crack inclination θ and with a size $a = 15$ mm. It can be seen that the K_{II} values increase starting from 0 reaching the maximum at the inclination value about $\theta \approx 45^\circ$. Then, these curves start decreasing differently once the angular value exceeds 45° ($\theta > 45^\circ$), it all depends on the properties of adhesive and shapes of the patches.

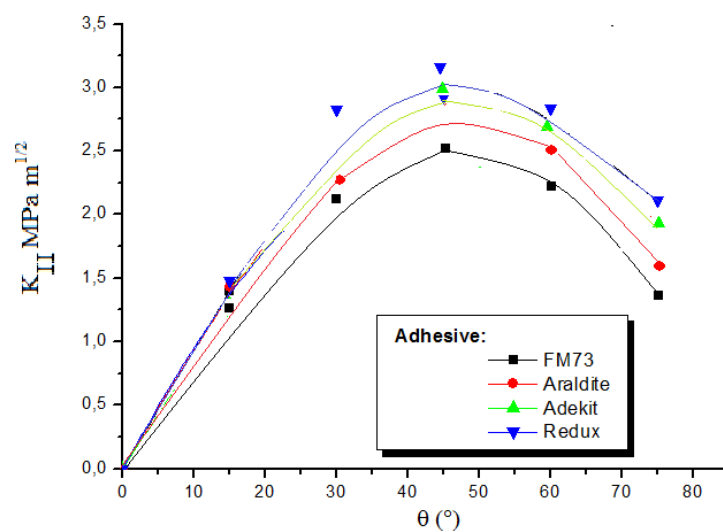


Fig. 16 SIF vs the crack inclination θ of mode II for elliptical shape patch

The curves are almost the same for all adhesives types, after studying the curves we note that the K_{II} values are close, except that the FM73 adhesive gives the lowest values of SIF (K_{II}), and this clearly indicates that this adhesive relieves stresses at the crack level better, thus presenting the energy gain which equals 16 % for adekit and 15 % for redux, this difference tends towards 0 for $\theta = 90^\circ$ and $\theta = 0^\circ$.

Variation of stress intensity factor SIF (K_I+K_{II}) according to the crack inclination θ for different adhesive types

The stress intensity factor study of the sum of SIFs ($K_I + K_{II}$) was presented as a function of the crack inclination θ in Fig. 3, it is evident that ($K_I + K_{II}$) values decrease with increasing crack inclination, regardless of the composite shape or the type of adhesive. We note that the (araldite, redux and adekit) curves have the same behavior, because the difference in the values of the SIFs ($K_I + K_{II}$) is very small compared to FM73 adhesive. The energy gain of these results is returned: ($\theta = 0^\circ$) 29 % and ($\theta = 75^\circ$) 37 % on average compared to the other three types of adhesives.

The redux glue was the worst compared to all other types of adhesives used in this study, with the ($K_I + K_{II}$) values being very high. SIF varies between (10 to 7.5 MPa m). The curves of Fig. 17 show that FM73 glue gives the lowest values of $K_I + K_{II} = 3.5 \text{ MPa}\cdot\text{m}^{1/2}$, indicating its effectiveness. From it we conclude that FM73 glue is the most efficient in this study.

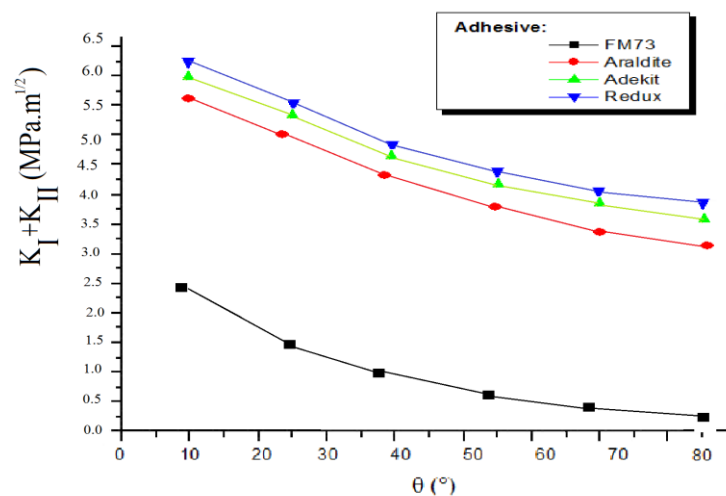


Fig. 17. K_I and K_{II} vs the crack inclination θ for different adhesive type

Ultimate strength and stiffness depending on the patch type

In this experimental study we used AL 2024 aluminum alloy. To obtain the appropriate samples for the experiment, we accelerate the corrosion using water + salt basins, and then immerse these plates in this solution, and then we cut the AL2024 alloy into several samples. These samples have a rectangular shape with dimensions (200 × 150 × 3) mm³.

Aluminum is naturally covered with a layer of oxide, which often protects it from corrosion. In neutral aqueous solutions (4 < pH < 9), this oxide film is 50 Å thick and protects the metal (passivation), but chloride (Cl) ions have a very destabilizing effect on this oxide layer, then a rupture of the oxide layer occurs, which leads to corrosion.

Figures 18 and 19 show the completed stages in which we obtained corroded aluminum plates. To confirm the results obtained in the analytical study, we conducted an experimental study on AL 2024 aluminum alloy. To obtain the appropriate corroded samples for the experiment, we accelerate the corrosion using water + salt basins, and then immerse these plates in this solution, and then we cut the AL2024 alloy into several samples. These samples have a rectangular shape with dimensions $(200 \times 150 \times 3) \text{ mm}^3$ (Fig. 20).

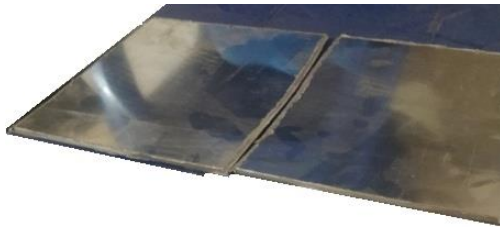


Fig. 18 Before the process



Fig. 19 Three weeks after the operation



Fig. 20 Geometry of the repaired specimens

Aluminum is naturally covered with a layer of oxide, which often protects it from corrosion. In neutral aqueous solutions ($4 < \text{pH} < 9$), this oxide film is 50 \AA thick and protects the metal (passivation), but chloride (Cl) ions have a very destabilizing effect on this oxide layer, leading to corrosion.

According to the ASTM D3039-76 [30], ultimate strength is obtained. The ASTM D3039 tensile test is used to measure the force required to break a composite sample and how far the sample stretches or elongates to that breaking point. Tensile testing produces a stress–strain diagram which is used to determine the tensile modulus.

The objective of this pilot study was to analyze the absolute strength as a function of the types of adhesives (FM73, redux, araldite and adekit) for fixing the rectangular-shaped boron/epoxy patch used to repair the corroded aluminum plate.

This study proved that the use of composite materials increases the value of the absolute strength of the aluminum plate so that the untreated corroded plate fails with a value of only 100 MPa, while using composite materials, this value increased to reach

the value of 150 MPa when using the graphite / epoxy adhesive, 188 MPa for redux, 190 for araldite and 220 MPa for boron/epoxy adhesive.

After observing the obtained values, it can be concluded that FM73 adhesive has effective effect and high stress transfer efficiency compared to other materials (redux, araldite and adekit) with an increase of 16 % compared to araldite, 30 % redux and 45 % graphite which allows us to say that The FM73 adhesive is the best type of adhesive compared to other materials used in this work (Fig. 21).

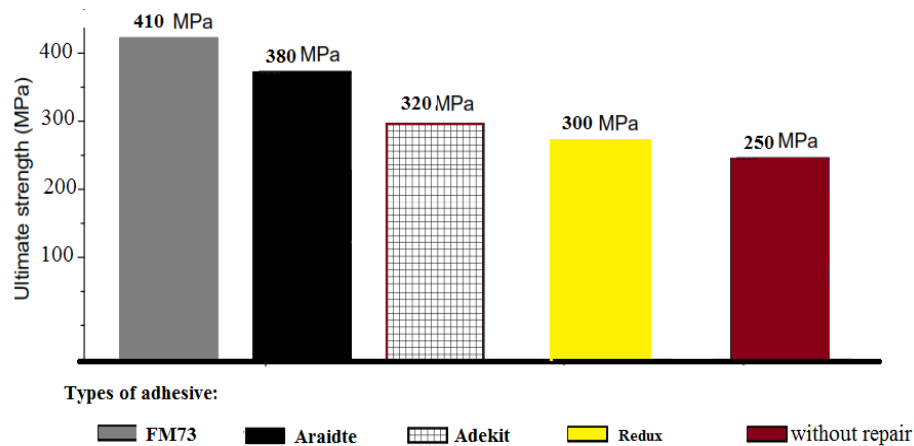


Fig. 21. Ultimate strength depending the type of adhesive for Al2024 aluminum plate on $T = 20\text{ }^{\circ}\text{C}$

Conclusions

This study made it possible to understand the corrosion behavior of 2000 series aluminum alloy under mechanical influence. This work focused in particular on aluminum alloy 2024-T4 with inclined crack, consists of two parts: a numerical analytical part and an experimental part. The analytical part, using the finite element method focused on evaluating the damaged area of several adhesives (FM73, araldite, adekit and redux) used in patch fixation, determining the stress intensity factor and then comparing the results for the different adhesive types. In the experimental part, we compared the ultimate tensile strength of the damage of corroded aluminum sheets that were repaired by boron / epoxy patch with several adhesive types.

This study allowed us, both on the analytical and experimental side, to conclude that FM73 adhesive is more efficient and effective compared to other adhesives (araldite, adekit and redux), because in the analytical study it gives the lowest values of the damaged area ratio of adhesive, the stress intensity factor, yither in mode I or mode II. As for the experimental study, it gives greater resistance to tensile strength and longer life compared to other adhesives.

References

1. Baker AA, Chester RJ. Recent advances in bonded composite repair technology for metallic aircraft components. In: *Proceeding of the International Conference on Advanced Composite Materials*. 1993. p.45-49.
2. Toudeshky HH. Effects of composite patches on fatigue crack propagation of single-side repaired aluminum panels. *Composite Structures*. 2006;76(3): 243–251.
3. Chung KH, Yang WH. A study of the fatigue crack growth behaviour of thick aluminium panels repaired with a composite patch. *Composite Structures*. 2003;60(1): 1–7.

4. Toudeshky HH, Sadeghi G, Daghyani HR. Experimental fatigue crack growth and crack-front shape analysis of asymmetric repaired aluminium panels with glass-epoxy composite patches. *Composite Structures*. 2005;71(3): 401–406.
5. Seo DC, Lee JJ, Daghyani HR. Fatigue crack growth behaviour of cracked aluminium plate repaired with composite patch. *Composite Structures*. 2003;57(1): 323–330.
6. Bassetti A. *Lamelles précontraintes en fibres de carbone pour le renforcement de ponts rivetés endommagés par fatigue*. Lausanne, Switzerland: EPFL; 2001.
7. Naboulsi S, Mall S. Fatigue growth of adhesively repaired panel using perfectly and imperfectly composite patches. *Theoretical and Applied Fracture Mechanics*. 1997;28(1): 13–28.
8. Sabelkin V, Mall S, Hansen MA, Vanderwaker RM, Derriso M. Investigation into cracked aluminium plate repaired with bonded composite patch. *Composite Structures*. 2007;79(1): 55–66.
9. Crocombe A, Richardson G. A unified approach for predicting the strength of cracked and non-cracked adhesive joints. *Int J Adhes*. 1995;49(3-4): 211–244.
10. Sheppard A, Kelly D, Tong L. A damage zone model for the failure analysis of adhesively bonded joints. *International Journal of Adhesion and Adhesives*. 1998;18(6): 385–400.
11. Kemal Apalak M, Gulapalak Z, Gunes R. Thermal and geometrically nonlinear stress analyses of an adhesively bonded composite, tee joint with double support. *J Thermoplast Compos Mater*. 2004;17(1): 103–36.
12. Ban CS, Lee YH, Choi JH, Kweon JH. Strength prediction of adhesive joints using the modified damage zone theory. *Composite Structure*. 2008;86(1-3): 96–100.
13. Berrahou M, Bachir Bouiadjra B. Analysis of the adhesive damage for different patch shapes in bonded composite repair of corroded aluminum plate. *Structural Engineering and Mechanics*. 2016;59(1): 123-132.
14. Berrahou M, Salem M, Mechab B, Bouiadjra BB. Effect of the corrosion of plate with double cracks in bonded composite repair. *Techno. Press*. 2017;64(3): 323-328.
15. Salem M, Berrahou M, Mechab B, Bouiadjra BB. Effect of the angles of the cracks of corroded plate in bonded composite repair. *Frattura ed Integrità Strutturale*. 2018;46(46): 113-123.
16. Berrahou M, Salem M, Belaïd M. Analysis of the plate failure repaired by composite patch and reinforced by stiffeners. In: *1st Conference on Renewable Energies & Advanced Materials ERMA'19 – Relizane, Algeria*. 2019; 276-280.
17. Salem M, Berrahou M, Mechab B, Bachir Bouiadjra B. Analysis of the adhesive damage for different patch shapes in bonded composite repair of corroded aluminum plate under thermo-mechanical loading. *Journal of Failure Analysis and Prevention*. 2021;21: 1274–1282.
18. Amari K, Berrahou M. Experimental and Numerical Study of the Effect of Patch Shape for Notched Cracked Composite Structure Repaired by Composite Patching. *Journal of Failure Analysis and Prevention*. 2022;22: 1040–1049.
19. Benzineb H, Berrahou M, Serier, M. Analysis of the adhesive damage for different shapes and types patch's in corroded plates with an inclined crack. *Frattura ed Integrità Strutturale*. 2022;16(60): 331-345.
20. M'hamdia R, Bachir Bouiadjra B, Serier B, Ouddad W, Feaugas X, Touzain S. Stress intensity factor for repaired crack with bonded composite patch under thermo-mechanical loading. *J Reinf Plast Compos*. 2011;30(5): 416–424.
21. Cetisli F, Kaman M. Numerical analysis of interface crack problem in composite plates jointed with composite patch. *Steel Compos Struct*. 2014;16(2): 203–220.
22. Bachir Bouiadjra B, Fari Bouanani M, Albedah A, Benyahia F, Es-Saheb M. Comparison between rectangular and trapezoidal bonded composite repairs in aircraft structures. *Mater Des*. 2011;32: 3161–3166.
23. Ruoyuliu T, Lingzhen L, Kazuo T. A partial stress intensity factor formula for CFRP repaired steel plates with a central crack. *Journal of Constructional Steel Research*. 2019;152: 105755.
24. *ABAQUS standard/user's manual, version 6.5*. Pawtucket, RI, USA: Hibbit Karlsson & Sorensen, Inc.; 2007.
25. Soboyejo WO. *Mechanical Properties of Engineered Materials*. Marcel Dekker; 2003.
26. Janssen M, Zuidema J, Wanhill R. *Fracture Mechanics: Fundamentals and Applications*. London; CRC Press; 2014.
27. Suresh S. *Fatigue of Materials*. Cambridge University Press; 2004.
28. Rooke DP, Cartwright DJ. *Compendium of stress intensity factors*. HMSO Ministry of Defence. Procurement Executive; 1976.
29. Sih GC, Paris PC, Erdogan F. Crack-tip stress intensity factors for the plane extension and plate bending problem. *Journal of Applied Mechanics*. 1962;29: 306–312.
30. ASTM Standard. *Standard test method for tensile properties of fiberresin composites D 3039-76*. Philadelphia: American Society for Testing and Materials; 1990.